2018

Differential-Mobility Spectrometry of 1-Deoxysphingosine Isomers: New Insights into the Gas Phase Structures of Ionized Lipids

Berwyck L. J Poad
Queensland University of Technology, bpoad@uow.edu.au

Alan T. Maccarone
University of Wollongong, alanmac@uow.edu.au

Haibo Yu
University of Wollongong, hyu@uow.edu.au

Todd W. Mitchell
University of Wollongong, toddm@uow.edu.au

Essa M. Saied
Humboldt Universität zu Berlin, Suez Canal University

See next page for additional authors

Publication Details

Poad, B. L. J., Maccarone, A. T., Yu, H., Mitchell, T. W., Saied, E. M., Arenz, C., Hornemann, T., Bull, J. N., Bieske, E. J. & Blanksby, S. J. (2018). Differential-Mobility Spectrometry of 1-Deoxysphingosine Isomers: New Insights into the Gas Phase Structures of Ionized Lipids. Analytical Chemistry, 90 (8), 5343-5351.

Differential-Mobility Spectrometry of 1-Deoxysphingosine Isomers: New Insights into the Gas Phase Structures of Ionized Lipids

Abstract

Separation and structural identification of lipids remain a major challenge for contemporary lipidomics. Regioisomeric lipids differing only in position(s) of unsaturation are often not differentiated by conventional liquid chromatography-mass spectrometry approaches leading to the incomplete, or sometimes incorrect, assignation of molecular structure. Here we describe an investigation of the gas phase separations by differential-mobility spectrometry (DMS) of a series of synthetic analogues of the recently described 1-deoxysphingosine. The dependence of the DMS behavior on the position of the carbon-carbon double bond within the ionized lipid is systematically explored and compared to trends from complementary investigations, including collision cross-sections measured by drift tube ion mobility, reaction efficiency with ozone, and molecular dynamics simulations. Consistent trends across these modes of interrogation point to the importance of direct, through-space interactions between the charge site and the carbon-carbon double bond. Differences in the geometry and energetics of this intramolecular interaction underpin DMS separations and influence reactivity trends between regioisomers. Importantly, the disruption and reformation of these intramolecular solvation interactions during DMS are proposed to be the causative factor in the observed separations of ionized lipids which are shown to have otherwise identical collision cross-sections. These findings provide key insights into the strengths and limitations of current ion-mobility technologies for lipid isomer separations and can thus guide a more systematic approach to improved analytical separations in lipidomics.

Disciplines

Medicine and Health Sciences | Social and Behavioral Sciences

Publication Details

Poad, B. L. J., Maccarone, A. T., Yu, H., Mitchell, T. W., Saied, E. M., Arenz, C., Hornemann, T., Bull, J. N., Bieske, E. J. & Blanksby, S. J. (2018). Differential-Mobility Spectrometry of 1-Deoxysphingosine Isomers: New Insights into the Gas Phase Structures of Ionized Lipids. Analytical Chemistry, 90 (8), 5343-5351.

Authors

Berwyck L. J Poad, Alan T. Maccarone, Haibo Yu, Todd W. Mitchell, Essa M. Saied, Christoph Arenz, Thorsten Hornemann, James Bull, Evan J. Bieske, and Stephen J. Blanksby

Differential-Mobility Spectrometry of 1-Deoxysphingosine Isomers: New Insights into the Gas Phase Structures of Ionized Lipids

Berwyck L. J. Poad[1*], Alan T. Maccarone[2, 3], Haibo Yu[3], Todd W. Mitchell[4], Essa M. Saied[5,6], Christoph Arenz[5], Thorsten Hornemann[7], James N. Bull[8], Evan J. Bieske[8], Stephen J. Blanksby[1*]

[1] Central Analytical Research Facility, Institute for Future Environments, Queensland University of Technology, Brisbane, QLD 4001, Australia, [2] Mass Spectrometry User Resource and Research Facility, University of Wollongong, Wollongong, NSW 2522, Australia, [3] School of Chemistry, University of Wollongong, Wollongong, NSW 2522, Australia, [4] School of Health Science, University of Wollongong, Wollongong, NSW 2522, Australia, [5]Institute for Chemistry, Humboldt Universität zu Berlin, 12489 Berlin, Germany, [6]Chemistry Department, Faculty of Science, Suez Canal University, 41522 Ismailia, Egypt, [7]Institute of Clinical Chemistry, University and University Hospital of Zurich, CH-8091 Zurich, Switzerland, [8]School of Chemistry, University of Melbourne, Parkville, VIC 3010, Australia.

KEYWORDS Ion Mobility, Lipids, Molecular Dynamics, Ozonolysis.

ABSTRACT: Separation and structural identification of lipids remains a major challenge for contemporary lipidomics. Regioisomeric lipids differing only in position(s) of unsaturation are not differentiated by conventional liquid chromatography-mass spectrometry approaches leading to the incomplete, or sometimes incorrect, assignation of molecular structure. Here we describe an investigation of the gas phase separations by differential mobility spectrometry (DMS) of a series of synthetic analogues of the recently described 1-deoxysphingosine. The dependence of the DMS behavior on the position of the carbon-carbon double bond within the ionized lipid is systematically explored and compared to trends from complementary investigations, including collision cross sections measured by drift tube ion mobility, reaction efficiency with ozone, and molecular dynamics simulations. Consistent trends across these modes of interrogation point to the importance of direct, through-space interactions between the charge site and the carbon-carbon double bond. Differences in the geometry and energetics of this intra-molecular interaction underpin DMS separations and influence reactivity trends between regioisomers. Importantly, the disruption and reformation of these intra-molecular solvation interactions during DMS are proposed to be the causative factor in the observed separations of ionized lipids which are shown to have otherwise identical collision cross sections. These findings provide key insights into the strengths and limitations of current ion-mobility technologies for lipid isomer separations and can thus guide a more systematic approach to improved analytical separations in lipidomics.

Electrospray ionization (ESI) mass spectrometry has become the leading technology for the identification and quantification of lipids in complex biological extracts.[1,2] Coupling ESI with high-resolution mass analysis and/or different configurations of tandem mass spectrometry can provide an information-rich snapshot of the lipids present within a tissue, cell or organism.[3,4] While such analyses are capable of describing a lipidome with many hundreds of lipid identifications, they also belie a greater molecular complexity arising from lipid isomers that – by definition – have the same exact mass and often have similar tandem mass spectral signatures. One common example of such isomerism is lipids that differ in the position or stereochemistry of the carbon-carbon double bond(s) within the aliphatic chain.[5] Conventional low energy (< 100 eV) collision-induced dissociation (CID) mass spectra of ionized lipids do not yield product ions that are diagnostic of the position or configuration of double bonds and thus, in the absence of ancillary information, lipid identification is incomplete and the presence of multiple isomers cannot be excluded.[6,7] Such ambiguity in lipid structure assignment can have significant consequences for the reliable elucidation of lipid biochemistry. In a recent study, some of us have demonstrated that in HEK293 cells, desaturation of 1-deoxysphinganine to produce 1-deoxysphingosine (1-deoxySO) occurs at the *n*-4 position[8] rather than the *n*-14 position predicted by the canonical mechanism for sphingolipid metabolism[9,10] (see structures in Figure 1). This discovery has implications for understanding the fate of 1-deoxysphingolipids in pathologies associated with aberrant lipid metabolism (*e.g.*, hereditary sensory neuropathy type 1)[11] along with the application of 1-deoxysphingolipids as disease markers (*e.g.*, type-2 diabetes).[12,13]

The sphingolipids shown in Figure 1 are isomers and thus cannot be discriminated based on mass-to-charge ratio (*m/z*). Moreover, the similarity in the CID spectra of these species further impedes unique structural assignment. In our previous study,[8] 1-deoxySO (*n*-4) was unambiguously identified by a unique combination of differential-mobility spectrometry (DMS)[14] and ozone-induced dissociation (OzID).[15] This is one example from a growing body of work indicating that ion-mobility spectrometry, in its various forms, is an important new tool for lipid isomer discrimination.[16,17] DMS,[18-20] classical drift-tube ion mobility[21-23] and travelling-wave mobility[24,25]

have all been demonstrated to be effective in separating different types of isomeric lipids. When used in conjunction with reference standards or alternative ion activation methods these mobility-based approaches can both improve confidence in lipid identification and elucidate the presence of multiple isomers. In order for the number of applications of ion-mobility technology in lipidomics to continue expanding, the fundamental physicochemical principles underpinning these separations require further study. Indeed, scant attention has been paid to the structure and dynamics of ionized lipids in the gas phase. Such understanding is critical to reliably predict the efficacy of these approaches and to provide a framework for selection and optimization of ion-mobility methods in different lipidomics applications.

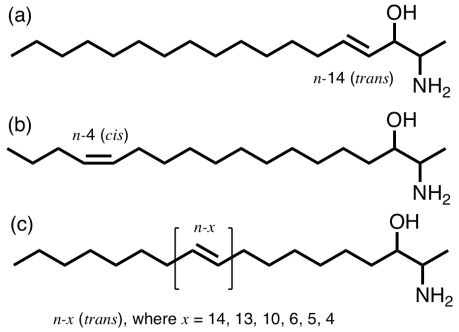

Figure 1: (a) Structure of 1-deoxysphingosine, 1-deoxySO (*n*-14, *trans*), predicted by the canonical pathways of sphingolipid biosynthesis with a *trans* double bond in the *n*-14 (Δ4) position. (b) Structure of native 1-deoxysphingosine, 1-deoxySO (n-4, *cis*), identified by Steiner *et al*. with a *cis* double bond in the *n*-4 (Δ14) position.[8] (c) Sites of unsaturation for the 1-deoxysphingosine *trans* isomeric standards used in this work.

Kim and co-workers undertook the most comprehensive study to-date of the gas phase structure of ionized lipids by measuring the drift times of a homologous series of ionized phosphatidylcholines on a travelling-wave ion-mobility mass spectrometer.[24,25] For saturated lipids, these experiments revealed a strong correlation between mobility and mass, suggesting a lack of significant intra-molecular interactions in the structures of the gas phase ions. Significantly, the introduction of a single point of unsaturation in the acyl chains of a phosphatidylcholine resulted in a deviation from this trend with a reduction in drift time of *ca*. 5%. Molecular dynamics simulations showed that the *cis* carbon-carbon double bond induced a bent configuration in most low-energy structures, suggesting a possible cause for the deviation from the prevailing mass-dependent trend for the saturated lipids. To extend this discovery and optimize mobility-based separation of isomeric lipids, it is important to understand how the location of the carbon-carbon double bond affects the structure and dynamics of ionized lipids. In the present study, we have used DMS and drift-mobility to examine the behavior of a homologous series of synthetic deoxysphingosines that differ only in the location of the carbon-carbon double bond. Molecular dynamics simulations are used to explore the three-dimensional structure of the ionized lipids in the gas phase. These calculations highlight specific charge-olefin interactions that could be responsible for different mobility behaviors. Calculations are supported by gas phase ion-molecule reactions between the ionized lipids and ozone revealing a strong influence of the double bond location and stereochemistry on reaction efficiency.

METHODS

Sample preparation: 1-deoxysphingosine, (2*S*,3*R*,14*Z*)-2-aminooctadec-14-en-3-ol (1-deoxySO (*n*-4, *cis*)) was synthesized as described previously.[8] Six regioisomers, 1-deoxySO (*n*-4, *trans*); 1-deoxySO (*n*-5, *trans*); 1-deoxySO (*n*-6, *trans*); 1-deoxySO (*n*-10, *trans*); 1-deoxySO (*n*-13, *trans*) and; 1-deoxySO (*n*-14, *trans*) were synthesized by a procedure that will be reported in a subsequent publication. A commercial standard of 1-deoxysphinganine (1-deoxySA) was purchased from Avanti Polar Lipids (Alabaster, AL, USA).

Differential-Mobility Mass Spectrometry: Mass spectra were acquired using a 5500 QTRAP mass spectrometer previously modified to allow introduction of ozone into the collision cell, equipped with a commercially available Differential Mobility Spectrometer (SelexIon™ SCIEX, Concord, Ontario, Canada). This DMS module attaches in the source region of the instrument and comprises two parallel plates to which a high-voltage asymmetric radio-frequency (RF) potential is applied, dispersing the ionized molecules by their interaction with this asymmetric RF field.[26] A DC Compensation Voltage (COV) is then applied to selectively introduce the dispersed ions into the mass spectrometer. Standards of 1-deoxysphingosine and 1-deoxysphinganine were made up to 0.1 μM concentration in methanol (LCMS Grade, VWR Scientific, Murrarie, QLD, Australia) with 5 mM ammonium acetate (UPLC grade, Sigma Aldrich, St Louis MO).

Ozone-induced Dissociation (OzID) spectra were acquired using a modified method table that enabled the collision cell to be filled with mass-selected ions and trapped in the presence of ozone for pre-defined periods.[18,27] Ozone was produced by an external generator (Titan30, Absolute Ozone, Alberta, Canada) operating at 220 gm^{-3} (14.7% w/w ozone in oxygen). A small portion of this gas was directed into the mass spectrometer through a variable leak valve (Nenion, Lustenau, Austria) and mixed into the N_2 collision gas. Following ozonolysis, ions were transferred to the third quadrupole region for mass analysis. A schematic of the ozone production and subsequent introduction to the mass spectrometer is provided in the Supporting Information (Figure S1) along with the typical operating parameters (Table S1).

Differential mobility spectra (DMS) were acquired by ramping the COV using a fixed separation voltage (SV) of 4200 V while acquiring OzID mass spectra. The DMS device was stabilized for at least 60 mins prior to data acquisition. For some experiments, LCMS grade propan-2-ol was used as a modifier reagent in the DMS gas with a feed rate of 150 μL min^{-1}.

Drift Tube Ion Mobility Spectrometry Collision cross sections of protonated 1-deoxysphingosine ions were measured using a custom ion mobility spectrometer that has been described in detail previously.[28] The mobility resolution of this instrument has been shown to be $t/\Delta t \sim 80$ for singly charged ions, where t is the mean arrival time and Δt is the full-width half-maximum of the arrival time distribution.[28] Collision cross sections were determined using a previously reported procedure,[29] which involved extrapolation of the median arrival time as a function of the potential field drop across the second of two drift stages. For calibration and comparison with other measurements, the collision cross section of tetrabutylammonium cations (*m/z* 242) was periodically measured and consistently found to be ~2 $Å^2$ above the accepted value of 242.5 $Å^2$.[30] Further details for the drift mobility experiments are provided in the Supporting Information.

Molecular dynamics simulations. Molecular dynamics (MD) simulations of six 1-deoxysphingosine isomers in the gas phase were carried out using CHARMM.[31] The 1-deoxysphingosine molecules were represented with DFTB3.[32] In total, all 58 atoms were treated quantum mechanically. The dispersion corrected DFTB3 method was used as it provides an improved description for hydrogen bonding systems.[33-35] The utilization of the highly efficient approximate DFTB3 method circumvents the need for development of classical force fields, while at the same time its performance allows a reasonable conformational sampling. The time-step was chosen to be 1 fs and Langevin dynamics was solved with a friction coefficient of 5 ps^{-1} assigned to all the heavy atoms. The temperature was maintained at 298 K to mimic the experimental conditions. In order to speed up the convergence in conformational sampling, 20 independent simulations starting from a different structure were carried out each for 10 ns. In total, 1.2 μs simulations were carried out. The trajectories were saved every 10 ps for further analyses.

Theoretical determination of cross sections. The cross sections for the MD-sampled structures were calculated using the MOBCAL software[36] with the optimized parameters for ion mobility experiments in nitrogen gas.[25,37] The trajectory method[36] was adopted as it has been shown to provide the most accurate prediction. The cross section was calculated for structures sampled every 100 ps, thus for each simulation there are 2,000 structures. The partial charges based on the CGenFF force field[38] were assigned to each atom for the MOBCAL calculations using the paramchem interface (https://cgenff.paramchem.org/).

RESULTS

Separation and identification of 1-deoxySO isomers by DMS and OzID: Figure 2(a) shows an ionogram of a compensation voltage (COV) ramp for the $[M+H]^+$ ion of 1-deoxySO (*n*-4, *trans*) at *m/z* 284.3; with the separation voltage set to +4200 V the total ion chromatogram (TIC) abundance peaks around 17.3 V. Repeated mass selection and trapping of this precursor ion in the presence of ozone while scanning the compensation voltage allowed unambiguous identification of the double bond position, with OzID product ions diagnostic for the *n*-4 double bond position apparent in Figure 2(b). The extracted ion chromatogram (XIC, indicated by red squares in Figure 2a) shows that the DMS behavior of these OzID product ions tracks the behavior of the precursor ion. Using identical DMS settings, the ionogram of a mixture of the 1-deoxySO (*n*-4, *trans*) and 1-deoxySO (*n*-10, *trans*) regioisomers (Figure S2a) showed very similar COV behavior, with the peak TIC abundance around 17.8 V, albeit with a slightly wider peak shape. This peak broadening is a good indication that the differential mobility of these two isomers is not identical. Extracting the OzID product ions for the two isomers shows this, with the ions diagnostic for the 1-deoxySO (*n*-4, *trans*) isomer appearing at slightly lower COV than those corresponding to the 1-deoxySO (*n*-10, *trans*) isomer. In previous OzID studies, it has been noted that the rate of the ozonolysis reaction is influenced by the proximity of the site of unsaturation to the charge, with slower reaction rates observed for olefins closer to the charged moiety along the hydrocarbon chain.[27,39] This decrease in reaction rate is apparent in Figure S2(b), with the OzID product ions for the 1-deoxySO (*n*-10, *trans*) isomer detected in much lower relative abundance than those of the 1-deoxySO (*n*-4, *trans*) isomer.

In addition to the site of unsaturation, the stereochemistry of the double bond (*i.e.*, *cis* or *trans* configuration) has been shown to influence the ion-mobility behavior[23] and the gas-phase reaction rate of ozone with an unsaturated lipid.[27,40,41] To explore this trend, DMS and OzID experiments were conducted using the 1-deoxySO (*n*-4, *cis*) and 1-deoxySO (*n*-4, *trans*) isomers. While some DMS separation between the individual injections of each isomer could be inferred (as shown in Figure S3 of the Supporting Information), the isomers were not able to be resolved when infused as a mixture. Representative OzID mass spectra obtained from the stereoisomers (Figure S4) reveal OzID product ions consistent with the (*n*-4) site of unsaturation (see Table S2). Interestingly, the integrated OzID product ion abundance for the *trans* isomer was found to be 1.8 times larger than for the *cis* isomer, indicating a higher rate of ozonolysis in the former case. In addition the OzID product ions corresponding to the addition of atomic oxygen, $[1\text{-deoxySO+H+16}]^+$ (*m/z* 300.2), and the addition of molecular oxygen with a concomitant loss of water, $[1\text{-deoxySO+H+14}]^+$ (*m/z* 298.2), are also observed. For the *trans*-isomer, the peak area ratio of *m/z* 300/298 is 0.73, while for the *cis*-isomer the same ratio is just 0.44. This observed difference in the relative abundance of two

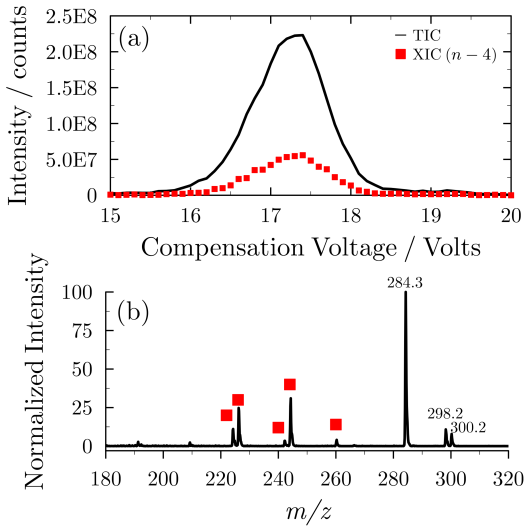

Figure 2: (a) DMS-OzID ionogram for the $[M+H]^+$ ion from 1-deoxySO (*n*-4, *trans*) showing the total ion chromatogram (TIC, black line) and extracted ion chromatogram (XIC, red squares) for the OzID product ions indicative of a *n*-4 double bond. (b) 1 s OzID mass spectrum from integrating 15 – 20 V in COV. Separation voltage was +4200 V and no chemical modifier was used for these experiments.

OzID product ions provides a sensitive marker for the stereochemistry of the double bond in this sphingolipid subclass. Indeed, re-analysis of the previously published OzID spectrum of 1-deoxySO derived from hydrolyzed HEK cell extracts reveals a peak area ratio of ~0.43.[8] This finding is in excellent agreement with the 1-deoxySO (*n*-4, *cis*) isomer and independently confirms the stereochemistry of the endogenous lipid that was assigned previously based on liquid chromatography retention time.[8]

Structure-mobility behaviors of ionized 1-deoxySO isomers in DMS: In order to enhance the separation between isomers, it is important to understand the relationship between molecular structure and DMS behavior. To investigate this relationship a homologous series of six synthetic 1-deoxySO isomers, with sites of unsaturation ranging from *n*-4 to *n*-14, all with *trans* configuration, were examined by DMS. Figure 3(a) shows the effect of the double bond position on differential mobility for individual injections of the *trans* *n*-4, *n*-5, *n*-6, *n*-10, *n*-13 and *n*-14 regioisomers of 1-deoxySO while maintaining the separation voltage at +4200 V. For the *n*-4, *n*-5 and *n*-6 isomers, a progressive shift to higher compensation voltage is observed with maximum values of 17.3, 18.7 and 19.6 V, respectively (Supporting Information, Table S3). For *n*-10 however, the compensation voltage for maximum transmission shifts back towards a lower COV of 17.7 V, and for the two isomers with the double bond closest to the charge, *n*-13 and *n*-14, the COV maximum occurs at 19.1 and 21.3 V, respectively (Supporting Information, Table S3). Although the six regioisomers have different COV maxima, no direct correlation of this voltage with the position of the carbon-carbon double bond within the hydrocarbon chain is apparent.

To explore this phenomenon further, the mobility of the two most extreme cases (*i.e.*, *trans* *n*-4 and *n*-14) were investigated across the full range of compensation and separation voltage space in both the presence and absence of the modifier propan-2-ol. The resulting dispersion plot shown in Figure 3(b) reveals

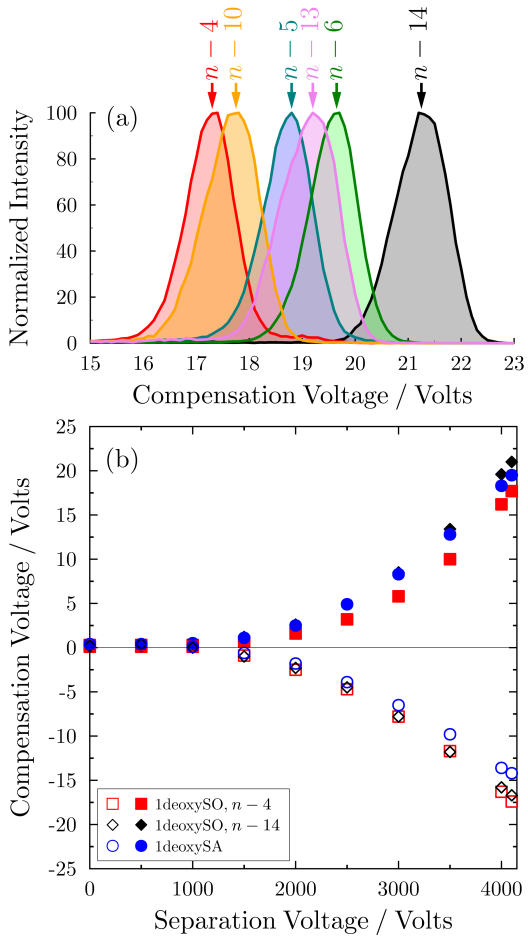

Figure 3: (a) Differential mobility spectrometry ionograms for the $[M+H]^+$ (*m/z* 284) ions derived from the 1-deoxySO isomers with double bond positions indicated by the *n-x* nomenclature (Figure 1). Normalized ion peak intensity is reported resulting from OzID acquisitions (1 s trapping times). Separation voltage used for these experiments was +4200 V. No chemical modifier was used and the DMS resolving gas pressure was 10 psi. (b) Dispersion plot for the DMS mobility of the monounsaturated *n*-4 (red squares) and *n*-14 (black diamonds) 1-deoxySO isomers along with the saturated 1-deoxysphinganine (blue circles). Experiments were conducted with no chemical modifier (solid points) and propan-2-ol (open points).

that, in the absence of any modifier, the compensation voltage required to transmit the $[M+H]^+$ cations from both 1-deoxySO isomers increases with increasing separation voltage, leading to a concomitant increase in the separation of the two isomers. This DMS behavior suggests that, under these conditions, the mobility of both isomers is dominated by hard-sphere collisions (often termed 'type C' mobility behavior) and pointing to possible differences in the three dimensional structures of the ionized lipid isomers in the gas phase.[26,42] Interestingly, examination of the $[M+H]^+$ cation derived from the fully saturated 1-deoxysphinganine (1-deoxySA) across the same voltage space shows that it tracks most closely with 1-deoxySO (*n*-14, *trans*) (Figure 3b). This observation suggests that the gas phase structure of ionized 1-deoxySO (*n*-4, *trans*) is more significantly impacted by the presence of the carbon-carbon double bond; perhaps an indication of the influence of through-space interactions of the charge with the site of unsaturation in defining the three-dimensional structure. The addition of propan-2-ol as a chemical modifier to the carrier gas results in negative compensation voltages for the transmission of all three ionized sphingolipids across the same separation voltage range, as illustrated in Figure 3(b). This mobility behavior indicates the participation of clustering (solvating) and de-clustering (desolvating) interactions between the ions and modifier vapor through the low- and high-field cycles of the separation waveform (termed 'type A' mobility behavior).[26,42] In the presence of the modifier, the dispersion plots of 1-deoxySO (*n*-4, *trans*) and 1-deoxySO (*n*-14, *trans*) are observed to be coincident and are both well separated from the saturated 1-deoxySA. One possible explanation for these results would be the role of the modifier in disrupting important intra-molecular interactions that results in a quenching of the mobility-based discrimination of the two isomers. Taken together, these observations hint at the position of the carbon-carbon double bond influencing the three-dimensional structure of the ionized 1-deoxySO isomers through charge-olefin interactions. It could follow then, that such interactions might manifest as a difference in collision cross section and consequently drift-tube ion mobility measurements of this homologous series of lipid isomers were undertaken.

Collisional cross section measurements of ionized 1-deoxySO isomers: The data described above show a marked change in DMS behavior between ionized 1-deoxySO isomers but this does not simply correlate with the site of unsaturation within the primary structure of the lipid. This raises the question as to whether the different sites of unsaturation lead to significant changes in the three-dimensional geometries of the ionized lipids in the gas phase? To investigate this hypothesis collision cross section measurements were undertaken for the $[M+H]^+$ cations of all six (*trans*) 1-deoxySO isomers using a home-built drift-tube ion mobility instrument operated with nitrogen buffer gas. The results are summarized in Figure 4 and show that collision cross sections for all isomers fall between the narrow range of 180 – 185 Å^2 such that no significant differences are identified within the uncertainty of the measurements. The scale of the uncertainty in these measurements results from the relatively low mobility resolution achieved for the ionized lipids. The resolution obtained for these singly charged lipids was typically $t/\Delta t \sim 50 - 60$; well below the instrument specification (see Supporting Information) and suggesting that the ion population for each isomer might constitute an ensemble of structures rather than a single, discrete gas phase geometry. While the interaction between the charge and olefin is also present in the drift mobility experiments and acts as a constraint on the molecular conformations adopted by the ions, the dominant influence on the collisional cross section is the phase space sampled by the remaining unconstrained portions of the hydrocarbon chain. To explore the conformational space occupied by the ionized lipids, molecular dynamics simulations of all six isomers were conducted using an approximate density functional theory (DFTB3) approach. Sampling the mean and standard deviations in collisional cross section determination across the ensemble of ion structures gave the results summarized in Figure 4.

The mean values for the theoretical cross sections agree well with the experimental determinations and show no significant variation between the isomers. This is also reflected in the tight distributions calculated for the dipole moments and isotropic polarizability of the isomers (see Figure S5 of the Supporting Information). Significantly, the relative standard deviations in the computed collision cross sections are large, *ca.* 5%, consistent with the broad distribution of structures inferred from the

experimental measurements. Both theory and experiment indicate that collision cross section is largely conserved between isomeric ions and is thus *not* the cause of isomer discrimination in DMS. An alternative explanation is that the DMS, unlike the drift mobility measurements, might be sensitive to the nature of through-space intra-molecular interactions between the charge and carbon-carbon double bond. The ensembles of structures predicted by molecular dynamics simulations provide a rich data set to explore this idea.

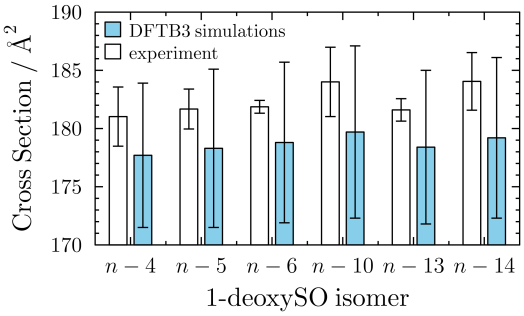

Figure 4: Collision cross sections for the $[M+H]^+$ ions of 1-deoxySO (*n*-*x*, trans) isomers (where *x* = 4, 5, 6, 10, 13 and 14) derived from experiment (white bars) and molecular dynamics simulations at the DFTB3 level of theory (blue bars). Experimental cross sections were determined from drift mobility measurements with an uncertainty largely arising from the broad arrival time distributions of these ions. Error bars on theoretical cross sections represent one standard deviation in the cross sections of all ion structures in the calculated ensemble.

Charge-olefin interactions in ionized 1-deoxySO isomers: In a previous DMS study of ionized phospholipids, intra-molecular solvation of the charge was postulated to play a critical role in the separation of different lipid classes.[19] The 1-deoxySO structures investigated here have a single site of protonation on nitrogen and present relatively simple systems to survey for interactions between the charge and the carbon-carbon double bond. The heat maps shown in Figure 5 plot the population density in the free energy landscape relative to the most populated conformation, with the phase space defined by: an average through-space distance between the proton on the ammonium charge carrier and each of the carbons of the double bond $\left(\frac{R_A+R_B}{2}\right)$ and the difference in the angles defined by the nitrogen and each of the carbons of the olefin $(\theta_A - \theta_B)$ where an angle of 0º indicates that the charged is sitting directly over the double bond (see Figure S6 in the Supporting Information). These representations show that for the $[M+H]^+$ ion populations of 1-deoxySO isomers (*n*-4, *trans*), (*n*-5, *trans*) and (*n*-6, *trans*) there exists a significant number of structures where folding of the hydrocarbon chain allows the ammonium charge carrier to be positioned directly over the carbon-carbon double bond and facilitates a proton-olefin distance of *ca*. 2.5 Å (Figure 5b, d, f). Representative structures from each of these populations are shown in Figure 5(a, c and e) and highlight the ammonium proton centered directly over the carbon-carbon double bond. For isomers with the double bond further from the methyl end of the hydrocarbon chain the number of structures adopting this ordered arrangement is far fewer. The *n*-10 isomer for example shows only a small population of structures adopting geometries with proton-olefin distances of 2.5 Å and angles close to 0° (Figure 5h). A representative *n*-10 geometry sampled from this region is shown in Figure 5(g) and indicates that, while the ion can adopt this conformation, the enthalpic and entropic penalties are too great for a significant population of such structures. In general, for protonated 1-deoxySO (*n*-10, *trans*) the molecular dynamics simulations do not identify a preferred geometry defined by a charge-olefin interaction. Interestingly however, where the through-bond distance between the double bond and the charge becomes even shorter, as for the *n*-13 and *n*-14 isomers, preferred geometries with significant numbers of ion structures re-emerge (Figure 5j and l). Noticeably however, these structures exhibit distinctly different interactions between the charge and olefin moieties. While these ensembles still have proton-double bond distances of between 2.5 – 3.0 Å the interactions are off-axis with differences in nitrogen-carbon-carbon bond angles of -60°. Representative structures from these regions are shown in Figures 5(i) and (k) and reveal the compact nature of these conformations required to facilitate the through-space integration of the ammonium moiety and the site of unsaturation when it is only 4 or 5 covalent bonds away. So, while the through-space charge-olefin distances are similar between the *n*-13/*n*-14 isomers and *n*-4/*n*-5/*n*-6 grouping, the significant differences in bond angle may indicate differences in the energetics and/or enthalpy of the interaction and thus predict distinctive influences in reactivity.

Structure-reactivity trends in the ozonolysis reactions of ionized 1-deoxySO isomers: The location of the double bond relative to the charged site in an ionized lipid has been previously shown to have a pronounced effect on the yield of OzID product ions; an indication of variation in reaction rate.[15,27] The homologous series of 1-deoxySO isomers however, present the first opportunity to systematically investigate this phenomenon. The summed abundance of the diagnostic OzID product ions as a proportion of the total integrated ion signal for each of the 1-deoxySO isomers obtained after a 1 s reaction time is shown in Figure S7 of the Supporting Information. These data reveal a striking effect of the position of the carbon-carbon double bond in the lipid and the efficiency of conversion of the $[M+H]^+$ precursor ion to ozonolysis products. For the 1-deoxySO (*n*-13, *trans*) and (*n*-14, *trans*) isomers, where the site of unsaturation is proximate in the chain to the ammonium charge carrier, OzID product ions constitute only 0.75 and 0.35% of the total ion abundance, respectively, after exposure to ozone for 1 s. The relatively slow rate of reaction of these monounsaturated lipids is consistent with previous anecdotal observations of low abundance OzID product ions arising from oxidative cleavage of the *n*-14 double bond in sphingosines[8] and glycosphingolipids.[39] In contrast, for the 1-deoxySO (*n*-4, *trans*), (*n*-5, *trans*) and (*n*-6, *trans*) isomers between 32 and 47% of the $[M+H]^+$ precursor ions are converted to products after 1 s in the presence of ozone. Interestingly, for 1-deoxySO (*n*-10, *trans*), where the double bond is located near the center of the hydrocarbon chain, the conversion to products is *ca.* 10%. Taken together these OzID data appear to cluster the six isomers into three groups namely, (1) 1-deoxySO (*n*-4, *trans*), (*n*-5, *trans*) and (*n*-6, *trans*) with highly efficient reactions at the olefin; (2) 1-deoxySO (*n*-13, *trans*) and (*n*-14, *trans*) with a sluggish rate of reaction and (3) 1-deoxySO (*n*-10, *trans*) with a response falling between the two extremes. Intriguingly, these groups of isomers are consistent with both the two different geometries of charge-olefin interaction, and the density of structures exhibiting these interactions, predicted by the molecular dynamics simulations. This consistency between the theoretical and experimental results also points to the through-space interaction between the ammonium cation and the carbon-carbon double bond as being critical

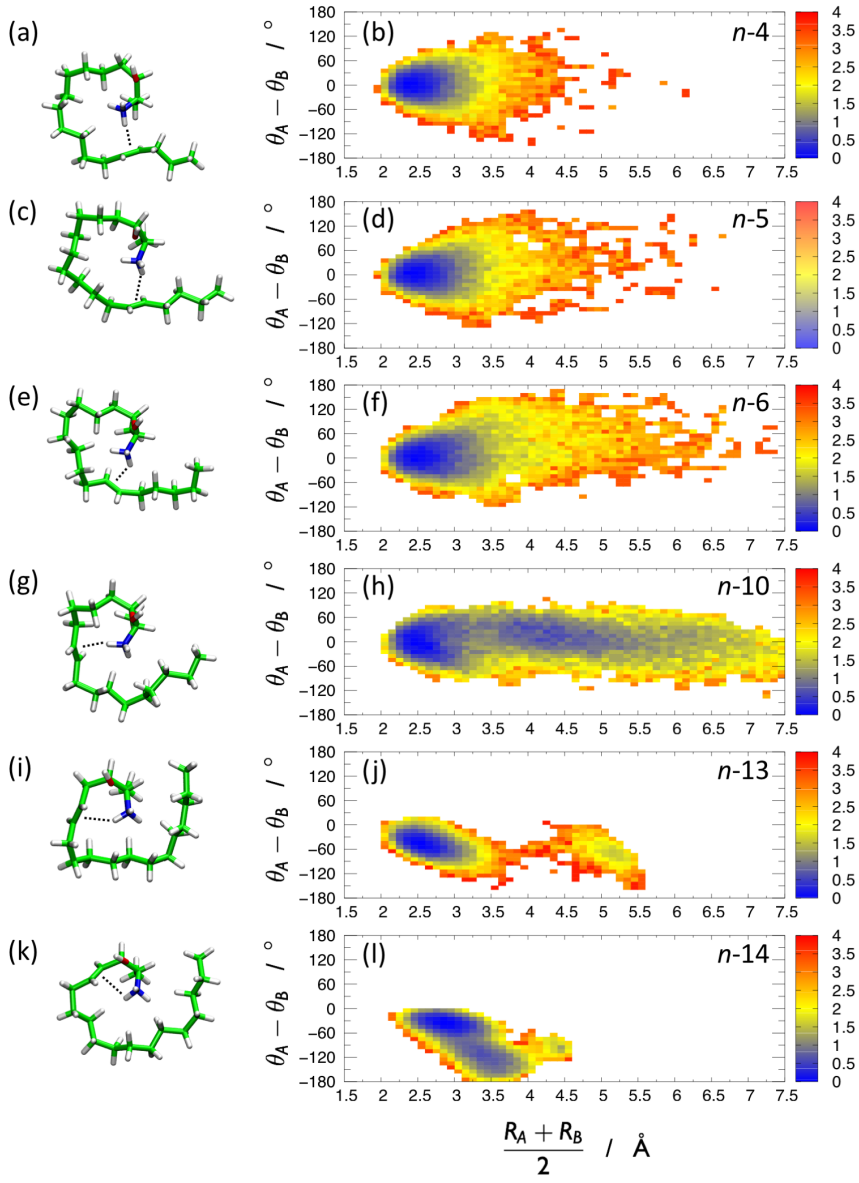

Figure 5: Free energy landscape for the $[M+H]^+$ ions of 1-deoxySO (*n*-*x*, trans) isomers (where $x = 4$, 5, 6, 10, 13 and 14) based on DFTB3 molecular dynamics simulations at 298 K. Structures are defined by the average through-space distance between the proton on the ammonium charge carrier and each of the carbons of the double bond and the difference in the angles defined by the nitrogen and each of the carbons of the olefin (see Figure S6 of the supporting information). The free energy difference (in kcal mol^{-1}) with respect to the most populated conformer is obtained through $\Delta G = -k_B T \ln \frac{p(i)}{p(lowest)}$ with k_B the Boltzmann constant, temperature T=298 K and $p(i)$ the probability of that particular conformer. Representative structures from the regions of greatest population density are shown for each of the isomers: (a, b) *n*-4; (c, d) *n*-5; (e,f) *n*-6; (g, h) *n*-10; (i,j) *n*-13; and (k, l) *n*-14.

to defining the DMS behavior of these ionized lipids and a means to rationalize the separations observed.

DISCUSSION

Kim and co-workers demonstrated that for complex lipids, the introduction of a site of unsaturation had a measurable effect on the collisional cross section of the gas phase ions corresponding to a contraction of approximately 5%.[24] In the present study, we have used a series of structurally simple lipid regioisomers to interrogate the effect of the *position* of unsaturation on the ionized lipid structure. Significantly, both the experimental measurements and theoretical predictions are in agreement that the different locations of the carbon-carbon double bond motif have no significant effect of collision cross section of the gas phase ion (*cf.* Figure 4). This is because, in the absence of strong intramolecular interactions, the ionized lipids explore a large conformational space with the unconstrained hydrocarbon chains largely responsible for defining the relatively large average collision cross section across these structural ensembles. Taken in isolation, it would be tempting to conclude from these results that ion-mobility is unlikely to have utility in affecting separations of isomeric lipids differing only in the position(s) of unsaturation. Closer inspection of the molecular dynamics simu-

lations however, indicates that for ionized 1-deoxySO the preponderance of structures accessed by the simulation show interactions between the charge-bearing ammonium moiety and the olefin at distances of *ca.* 2.5 Å (Figure 5). The preference to adopt this through-space interaction is somewhat independent of the location of the position of unsaturation in the hydrocarbon chain. The position does however dictate the geometry of the interaction, namely, whether the ammonium proton is centered directly above the carbon-carbon double bond (as for *n*-4, *n*-5 and *n*-6) or whether it is an off-center interaction (as for *n*-13 and *n*-14). Of the six isomers investigated only the simulated structural ensemble for protonated 1-deoxySO (*n*-10, *trans*) seems to have no strong preference for a charge-olefin interaction.

Prior experimental measurements suggest that the non-covalent bonding interaction between an ammonium cation (NH_4^+) and a model olefin such as ethylene (CH_2CH_2) is approximately 42 kJ mol^{-1}.[43] Furthermore, electronic structure calculations predict that the preferred geometry of such a cluster has the proton from the ammonium cation centered about 2.9 Å above the π-bond.[43] Such an interaction is most consistent with the geometries predicted for the *n*-4, *n*-5 and *n*-6 isomers of 1-deoxySO and if the interaction energy is similar, this could explain the activation of the carbon-carbon double bond towards reaction with ozone as evident in Figure S7. Conversely, the off-axis charge-olefin interaction observed for *n*-13 and *n*-14 isomers, while clearly residing in a free energy well, may serve to raise the activation barrier to reaction with ozone which requires passage through a highly ordered interfacial transition state.[44] If the two types of interaction described can be considered as activating and de-activating towards ozonolysis then the intermediate reaction efficiency of the protonated 1-deoxySO (*n*-10, *trans*) isomer reflects the lack of preference in the structural ensemble to adopt either conformation. This could suggest that either (1) the reactivity of this isomer reflects what would be observed in the absence of charge (*i.e.*, similar to gas phase reactivity of corresponding neutral) or (2) the reaction proceeds through the small population of ions adopting the activating charge-olefin interaction and the slower rate results from the kinetic bottleneck in the remaining ion population reorganizing to the activated conformation. Explicit calculations of the transition state energies for ozonolysis for representative structures for these ensembles would enable differentiation between these possibilities but such complex calculations are beyond the scope of the current study. Significantly, the OzID reaction provides a sensitive probe to the nature of the charge-olefin interaction in this series of isomeric lipids and supports the different geometries (and thus energies) of interaction as predicted by the molecular dynamics simulations.

Building on the hypothesis that differences in the intra-molecular solvation of the charge can drive separations in DMS experiments,[19] we can consider the two extremes of 1-deoxySO (*n*-4, *trans*) and 1-deoxySO (*n*-14, *trans*) that are separated by compensation voltages of up to 4 V (see Figure 3b). The molecular dynamics simulations and ozonolysis reactions reveal significant differences in the geometry and energetics of the intra-molecular interactions in each of these isomers. As a result, the disruption and reformation of these interactions (*cf.* folding and unfolding) during the high- and low-field cycles of the DMS will likely be distinctive for each isomer thus facilitating separation across the voltage space. This contention is supported by the loss of isomer resolution in the presence of a modifying gas where strong inter-molecular clustering interactions between the propan-2-ol and the charged ammonium moiety dominate over subtle intra-molecular bonding (*cf.* Figure 3b). For the remaining isomers, the protonated 1-deoxySO (*n*-5, *trans*) and 1-deoxySO (*n*-6, *trans*) regioisomers were found at progressively higher compensation voltages than 1-deoxySO (*n*-4, *trans*). This trend is mirrored in the ozone reactivity trend for these isomers that also shows a gradual increase in the abundance of oxidation products from *n*-4 to *n*-6 (Figure S7). The molecular dynamics simulations group these three isomers together with each having a preference for intra-molecular interactions defined by a similar on-axis geometry of the ammonium and olefin. The subtle, but systematic, differences in the energetics of this intra-molecular clustering can thus rationalize the trends observed in both DMS and OzID behaviors. Similarly, the 1-deoxySO (*n*-13, *trans*) and 1-deoxySO (*n*-14, *trans*) can be considered as a subgroup defined by similarly low ozonolysis efficiency and a distinct, off-axis geometry describing the charge-olefin interaction. Within this grouping the two isomers can be well resolved by DMS which exploits the small differences in the energetics of intra-molecular clustering between the two isomers. Finally, the computed geometries of protonated 1-deoxySO (*n*-10, *trans*) show no clear preference for intra-molecular solvation of the charge by the carbon-carbon double bond. It might be surmised therefore that transmission of this ion population through the DMS is not strongly influenced by such interactions.

CONCLUSIONS

The complexity of the lipidome, arising in part from the presence of isomeric lipids, has driven significant technology development aimed at the separation and identification of these isomeric species. Ion-mobility spectrometry coupled to mass spectrometry has received substantial recent attention as a means of discriminating between lipid isomers that have otherwise very similar physicochemical properties. Both drift-tube ion mobility and differential-mobility spectrometry show significant promise for facile gas phase resolution of ionized lipid isomers but limitations in our understanding of the factors influencing such mobility-based separations are hampering a systematic optimization of these technologies. In order to understand how small changes in the molecular structure of a lipid influence its structure and reactivity of the corresponding gas phase ion, we have completed a systematic study of a homologous series of simple lipid isomers differing only in their positions of unsaturation. The DMS, drift-tube ion mobility and ozonolysis reactivity of the 1-deoxySO provide key insights into the structure and energetics of these ionized lipids in the gas phase. Together with molecular dynamics simulations we have shown that for simple monounsaturated lipid ions, the through-space interaction between the charged moiety and the carbon-carbon double bond is a critical determinant of the preferred structures adopted by the ion populations. Significantly, the overall change in the average collisional cross section of the ionized lipids is not significantly affected by intra-molecular solvation. This suggests discrimination of isomers differing in the position of a single double bond by conventional drift-tube ion mobility will be extremely challenging and will likely require resolution that is not readily available in commercial platforms.[45] In contrast, we show that DMS can afford such separations by exploiting the subtle differences in the geometry and energetics of intra-molecular charge-olefin interactions. While this study represents a significant advance in our understanding of these separations it would be difficult to extrapolate these findings to *a priori* pre-

dict or systematically enhance DMS separations of lipid isomers. Nonetheless the findings do suggest that the application of modifiers in such analyses is likely to be counterproductive as it is likely to quench the subtle intra-molecular interactions critical to the separations. Rather it might suggest that derivatization of lipids to enhance the intra-molecular charge-olefin interactions may provide a path to more efficient separations using DMS technologies.

ASSOCIATED CONTENT

Supporting Information

One supporting PDF file containing supporting experimental details, 4 supplementary tables and 7 supplementary figures accompanies this manuscript. This Supporting Information is available free of charge on the ACS Publications website.

NOTES

Data Archive: An archive of the raw data files used to create some of the figures in this manuscript can be accessed at https://data.researchdatafinder.qut.edu.au/dataset/1-deoxysphingosine-dms-data

AUTHOR INFORMATION

Corresponding Author

* berwyck.poad@qut.edu.au, stephen.blanksby@qut.edu.au

Author Contributions

The manuscript was written through contributions of all authors and all authors have given approval to the final version of the manuscript.

ACKNOWLEDGMENT

This work was supported through funding from the *Australian Research Council* (ARC) Discovery Program (DP140101237, DP150101715, DP150101427 and DP160100474) and through the ARC Linkage Scheme (LP110200648 with SCIEX). Some of the results reported in this manuscript were obtained in the Central Analytical Research Facility (CARF), operated by the Institute for Future Environments (QUT). Access to CARF is supported by funding from the Science and Engineering Faculty (QUT). This project was undertaken with the assistance of resources and services from the National Computational Infrastructure (NCI), which is supported by the Australian Government.

REFERENCES

(1) Ekroos, K. *Lipidomics: Technologies and applications*; Wiley VCH: Weinheim, Germany, 2012.
(2) Han, X. *Lipidomics: Comprehensive mass spectrometry of lipids*; John Wiley & Sons: Hoboken, NJ, 2016.
(3) Blanksby, S. J.; Mitchell, T. W. *Ann. Rev. Anal. Chem.* **2010**, *3*, 433-465.
(4) Ryan, E.; Reid, G. E. *Acc. Chem. Res.* **2016**, *49*, 1596-1604.
(5) Hancock, S. E.; Poad, B. L. J.; Batarseh, A.; Abbott, S. K.; Mitchell, T. W. *Anal. Biochem.* **2017**, *524*, 45-55.
(6) Thomas, M. C.; Mitchell, T. W.; Harman, D. G.; Deeley, J. M.; Murphy, R. C.; Blanksby, S. J. *Anal. Chem.* **2007**, *79*, 5013-5022.
(7) Mitchell, T. W.; Pham, H.; Thomas, M. C.; Blanksby, S. J. *J. Chrom. B* **2009**, *877*, 2722-2735.
(8) Steiner, R.; Saied, E. M.; Othman, A.; Arenz, C.; Maccarone, A. T.; Poad, B. L. J.; Blanksby, S. J.; von Eckardstein, A.; Hornemann, T. *J. Lipid Res.* **2016**, *57*, 1194-1203.
(9) Duan, J.; Merrill, A. H. *J. Biol. Chem.* **2015**, *290*, 15380-15389.
(10) Merrill, A. H. *Chem. Rev.* **2011**, *111*, 6387-6422.
(11) Penno, A.; Reilly, M. M.; Houlden, H.; Laurá, M.; Rentsch, K.; Niederkofler, V.; Stoeckli, E. T.; Nicholson, G.; Eichler, F.; Brown, R. H.; von Eckardstein, A.; Hornemann, T. *J. Biol. Chem.* **2010**, *285*, 11178-11187.
(12) Othman, A.; Saely, C. H.; Muendlein, A.; Vonbank, A.; Drexel, H.; von Eckardstein, A.; Hornemann, T. *BMJ Open Diabetes Res. Care* **2015**, *3*, e000073.
(13) Othman, A.; Bianchi, R.; Alecu, I.; Wei, Y.; Porretta-Serapiglia, C.; Lombardi, R.; Chiorazzi, A.; Meregalli, C.; Oggioni, N.; Cavaletti, G.; Lauria, G.; von Eckardstein, A.; Hornemann, T. *Diabetes* **2015**, *64*, 1035-1045.
(14) Schneider, B. B.; Covey, T. R.; Coy, S. L.; Krylov, E. V.; Nazarov, E. G. *Int. J. Mass Spectrom.* **2010**, *298*, 45-54.
(15) Thomas, M. C.; Mitchell, T. W.; Harman, D. G.; Deeley, J. M.; Nealon, J. R.; Blanksby, S. J. *Anal. Chem.* **2008**, *80*, 303-311.
(16) Kliman, M.; May, J. C.; McLean, J. A. *Biochim. Biophys. Acta, Mol. Cell. Biol. Lipids* **2011**, *1811*, 935-945.
(17) Paglia, G.; Kliman, M.; Claude, E.; Geromanos, S.; Astarita, G. *Anal. Bioanal. Chem.* **2015**, *407*, 4995-5007.
(18) Maccarone, A. T.; Duldig, J.; Mitchell, T. W.; Blanksby, S. J.; Duchoslav, E.; Campbell, J. L. *J. Lipid Res.* **2014**, *55*, 1668-1677.
(19) Lintonen, T. P.; Baker, P. R.; Suoniemi, M.; Ubhi, B. K.; Koistinen, K. M.; Duchoslav, E.; Campbell, J. L.; Ekroos, K. *Anal. Chem.* **2014**, *86*, 9662-9669.
(20) Bowman, A. P.; Abzalimov, R. T.; Shvartsburg, A. A. *J. Am. Soc. Mass Spectrom.* **2017**, *28*, 1552-1561.
(21) Jackson, S. N.; Wang, H.-Y. J.; Woods, A. S.; Ugarov, M.; Egan, T.; Schultz, J. A. *J. Am. Soc. Mass Spectrom.* **2005**, *16*, 133-138.
(22) Groessl, M.; Graf, S.; Knochenmuss, R. *Analyst* **2015**, *140*, 6904-6911.
(23) Kyle, J. E.; Zhang, X.; Weitz, K. K.; Monroe, M. E.; Ibrahim, Y. M.; Moore, R. J.; Cha, J.; Sun, X.; Lovelace, E. S.; Wagoner, J.; Polyak, S. J.; Metz, T. O.; Dey, S. K.; Smith, R. D.; Burnum-Johnson, K. E.; Baker, E. S. *Analyst* **2016**, *141*, 1649-1659.
(24) Kim, H. I.; Kim, H.; Pang, E. S.; Ryu, E. K.; Beegle, L. W.; Loo, J. A.; Goddard, W. A.; Kanik, I. *Anal. Chem.* **2009**, *81*, 8289-8297.
(25) Kim, H.; Kim, H. I.; Johnson, P. V.; Beegle, L. W.; Beauchamp, J. L.; Goddard, W. A.; Kanik, I. *Anal. Chem.* **2008**, *80*, 1928-1936.
(26) Schneider, B. B.; Nazarov, E. G.; Londry, F.; Vouros, P.; Covey, T. R. *Mass Spectrom. Rev.* **2016**, *35*, 687-737.
(27) Poad, B. L. J.; Pham, H. T.; Thomas, M. C.; Nealon, J. R.; Campbell, J. L.; Mitchell, T. W.; Blanksby, S. J. *J. Am. Soc. Mass Spectrom.* **2010**, *21*, 1989-1999.
(28) Adamson, B. D.; Coughlan, N. J. A.; Markworth, P. B.; Continetti, R. E.; Bieske, E. J. *Rev. Sci. Instrum.* **2014**, *85*, 123109.
(29) Coughlan, N. J. A.; Adamson, B. D.; Gamon, L.; Catani, K.; Bieske, E. J. *Phys. Chem. Chem. Phys.* **2015**, *17*, 22623-22631.
(30) May, J. C.; Goodwin, C. R.; Lareau, N. M.; Leaptrot, K. L.; Morris, C. B.; Kurulugama, R. T.; Mordehai, A.; Klein, C.; Barry, W.; Darland, E.; Overney, G.; Imatani, K.; Stafford, G. C.; Fjeldsted, J. C.; McLean, J. A. *Anal. Chem.* **2014**, *86*, 2107-2116.
(31) Brooks, B. R.; Brooks, C. L.; Mackerell, A. D.; Nilsson, L.; Petrella, R. J.; Roux, B.; Won, Y.; Archontis, G.; Bartels, C.; Boresch, S.; Caflisch, A.; Caves, L.; Cui, Q.; Dinner, A. R.; Feig, M.; Fischer, S.; Gao, J.; Hodoscek, M.; Im, W.; Kuczera, K., et al. *J. Comp. Chem.* **2009**, *30*, 1545-1614.
(32) Gaus, M.; Cui, Q.; Elstner, M. *J. Chem. Theory Comput.* **2011**, *7*, 931-948.
(33) Gaus, M.; Goez, A.; Elstner, M. *J. Chem. Theory Comput.* **2013**, *9*, 338-354.
(34) Riccardi, D.; Schaefer, P.; Yang, Y.; Yu, H.; Ghosh, N.; Prat-Resina, X.; König, P.; Li, G.; Xu, D.; Guo, H.; Elstner, M.; Cui, Q. *J. Phys. Chem. B* **2006**, *110*, 6458-6469.
(35) Yang, Y.; Yu, H.; York, D.; Cui, Q.; Elstner, M. *J. Phys. Chem. A* **2007**, *111*, 10861-10873.
(36) Mesleh, M. F.; Hunter, J. M.; Shvartsburg, A. A.; Schatz, G. C.; Jarrold, M. F. *J. Phys. Chem.* **1996**, *100*, 16082-16086.
(37) Campuzano, I.; Bush, M. F.; Robinson, C. V.; Beaumont, C.; Richardson, K.; Kim, H.; Kim, H. I. *Anal. Chem.* **2012**, *84*, 1026-1033.

(38) Vanommeslaeghe, K.; Hatcher, E.; Acharya, C.; Kundu, S.; Zhong, S.; Shim, J.; Darian, E.; Guvench, O.; Lopes, P.; Vorobyov, I.; Mackerell, A. D. *J. Comp. Chem.* **2010**, *31*, 671-690.
(39) Barrientos, R. C.; Vu, N.; Zhang, Q. *J. Am. Soc. Mass Spectrom.* **2017**, *28*, 2330-2343.
(40) Vu, N.; Brown, J.; Giles, K.; Zhang, Q. *Rapid Commun. Mass Spectrom.* **2017**, *31*, 1415–1423.
(41) Marshall, D. L.; Saville, J. T.; Maccarone, A. T.; Ailuri, R.; Kelso, M. J.; Mitchell, T. W.; Blanksby, S. J. *Rapid Commun. Mass Spectrom.* **2016**, *30*, 2351-2359.
(42) Guevremont, R.; Purves, R. W. *Rev. Sci. Instrum.* **1999**, *70*, 1370-1383.
(43) Meot-Ner, M.; Deakyne, C. A. *J. Am. Chem. Soc.* **1985**, *107*, 474-479.
(44) Vayner, G.; Addepalli, S. V.; Song, K.; Hase, W. L. *J. Chem. Phys.* **2006**, *125*, 014317.
(45) Wojcik, R.; Webb, K. I.; Deng, L.; Garimella, V. S.; Prost, A. S.; Ibrahim, M. Y.; Baker, S. E.; Smith, D. R. *Int. J. Mol. Sci.* **2017**, *18*, 183.

Table of Contents artwork